J. Fluid Mech. (1987), *vol.* 183, *pp.* 147–161
Printed in Great Britain

Oscillations of a gas in a closed tube near half the fundamental frequency

By R. ALTHAUS† AND H. THOMANN
Institut für Aerodynamik, Swiss Federal Institute of Technology, CH-8092, Zürich, Switzerland

(Received 9 August 1986)

The oscillations are driven by the sinusoidal motion of a piston at one end of the tube. Near half the fundamental frequency the first overtone, driven by nonlinear effects, becomes resonant. For small boundary-layer friction the amplitude of this resonant part is comparable with the non-resonant acoustic solution and shocks are formed. Theoretical results are compared with pressure signals measured at the closed end of the tube. The viscous effects are large for air at atmospheric pressure and the nonlinear effects remain small. Experiments with xenon, sulphurhexafluoride (SF_6) and Freon RC-318 (C_4F_8) were therefore conducted and shocks formed as predicted. The comparison of the nonlinear theory by Keller (1975) with the experiments shows very good agreement.

1. Introduction

Linear acoustic theory predicts

$$u(x,t) = u_A \frac{\sin(\omega x/a_0)}{\sin(\omega L/a_0)} \cos \omega t, \tag{1.1}$$

for the one-dimensional isentropic motion of a gas in a tube shown in figure 1. As usual, u is the fluid velocity, ω the frequency, a_0 the speed of sound in the undisturbed fluid, l the amplitude of the piston displacement and $u_A = \omega l$. At the fundamental frequency $\omega = \pi a_0/L$ of the tube and at its multiples, (1.1) fails and shock waves occur. If, on the other hand, $\omega = \pi a_0/2L$ is chosen, the amplitude of the piston velocity equals $\hat{u}$ in figure 1 and the linearized solution (1.1) can satisfy both boundary conditions. However, the first overtone, driven by the nonlinear effects, becomes resonant in this case and severely disturbs the linear solution (1.1). This is illustrated in figure 2 which shows the contribution of this resonant overtone to the pressure signal at the closed end.

For an inviscid fluid, shocks were first predicted by Galiev, Ilhamov & Sadykov (1970) for this case. Some observations are also reported by Zaripov & Ilhamov (1976). However, their piston drive generated strong higher harmonics of the piston velocity which must be taken into account if their results near half the fundamental frequency are used.

Keller (1975) published a theory, based on Chester's (1964) work, that takes viscosity into account and predicts shocks for small viscosity. This theory permits a comparison with the experiments reported in the present paper. Similar effects can be expected for a tube with an open end, as pointed out by Keller (1977), by Sturtevant & Keller (1978) and by Galiullin & Khalimov (1979). This case, however,

† Present address: Brown, Boveri & Cie, AG, CH-5400 Baden, Switzerland.

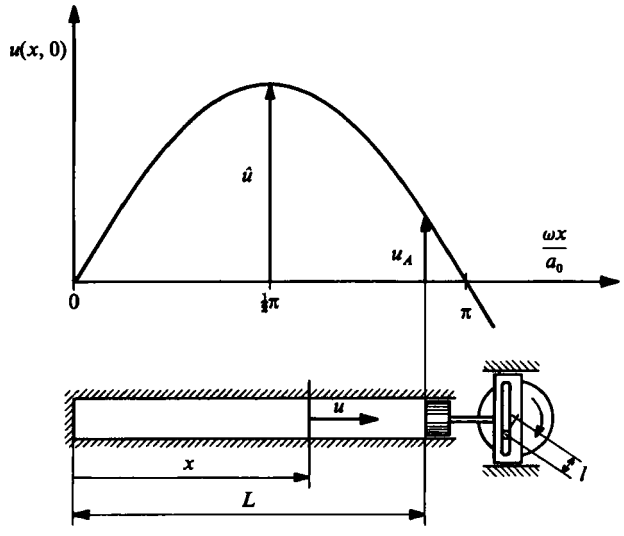

FIGURE 1. Velocity distribution in a tube, $u(L,t) = u_A \cos \omega t$.

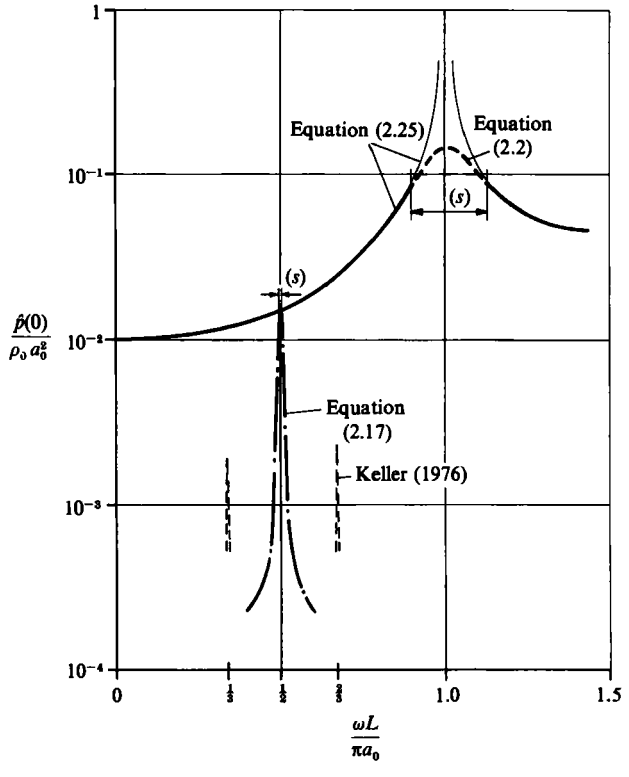

FIGURE 2. Contribution to the pressure signal at the closed end for $l/L = 10^{-2}$ and inviscid flow. Shocks are formed in (*s*). —·—, first overtone; ---, second overtone.

is less well defined as the details of the flow at the open end are unknown. Similar but weaker effects can also be expected at multiples $\frac{1}{3}$, $\frac{2}{3}$, $\frac{1}{4}$, etc., of the fundamental frequency (Keller 1976*b*). This result is supported by Mortell & Seymour (1981) who used a completely different approach. A survey of nonlinear acoustics is also given by Rott (1980).

The present paper is based on the thesis by Althaus (1986). It describes the experimental verification of Keller's (1975) predictions at half the fundamental frequency. For a comparison of this type it is crucial to use a carefully designed piston drive that generates a sinusoidal motion with extremely small higher harmonics. Calculated and measured pressure signals at the closed end are compared. Viscous effects dominate the resonant mode if air is used in the present arrangement. The heavy gases Freon RC-318 (C_4F_8), sulphurhexafluoride (SF_6) and xenon were therefore used to demonstrate the existence of shock waves and to check Keller's (1975) theory. Very good agreement between experiment and theory was found. Shock waves will also be observed for air at higher pressures.

2. Theory

2.1. *Oscillations near the fundamental frequency*

The unsteady one-dimensional flow of an isentropic fluid is described by the well-known set of equations

$$\left(\frac{\partial}{\partial t}+(u\pm a)\frac{\partial}{\partial x}\right)\left(u\pm\frac{2}{\gamma-1}a\right)=0, \tag{2.1}$$

where a is the local speed of sound and γ the specific heat ratio. Chester (1964) rearranges (2.1) and adds the contributions due to viscosity and conductivity. He assumes that the thickness of the Stokes boundary layer is small compared with the tube radius and that the wall temperature remains constant. For flow Mach numbers $\ll 1$ everywhere in the tube and for frequencies close to the fundamental ($\omega L/a_0-\pi \ll 1$), Chester's (1964) theory predicts

$$c-\tfrac{1}{2}\epsilon_c \sin\omega t = -\frac{4r_c}{\pi}\epsilon_c^{\frac{1}{2}}f(t)+f^2(t)-s_c\left(\frac{\omega\epsilon_c}{\pi}\right)^{\frac{1}{2}}\int_0^\infty f(t-\xi)\,\xi^{-\frac{1}{2}}\,\mathrm{d}\xi, \tag{2.2}$$

with

$$\epsilon_c = -\frac{4l}{(\gamma+1)\,L\cos(\omega L/a_0)}, \tag{2.3}$$

$$r_c = \frac{\pi a_0\tan(\omega L/a_0)}{(\gamma+1)\,\omega L\epsilon_c^{\frac{1}{2}}}, \tag{2.4}$$

$$s_c = \frac{2\beta}{\gamma+1}\left(\frac{\pi}{\omega\epsilon_c}\right)^{\frac{1}{2}}, \tag{2.5}$$

$$\beta = \frac{2}{R}\left(\frac{\nu_0}{\pi}\right)^{\frac{1}{2}}\left(1+\frac{\gamma-1}{Pr^{\frac{1}{2}}}\right), \tag{2.6}$$

and c a constant of integration. Here, R, ν_0 and Pr are the radius of the tube, the kinematic viscosity and the Prandtl number in the undisturbed gas. Several terms that are negligible for the conditions of the present experiments have been dropped from (2.2).

The unknown function f can be determined from (2.2). Results are given by Chester (1964) and by Keller (1976*a*). They predict shock waves for small r_c and s_c. The velocity $u(x,t)$ and the pressure disturbance $p(x,t)$ can be determined from the known solution f. There is

$$\frac{u(x,t)}{a_0} = f\left(t-\frac{x}{a_0}\right)-f\left(t+\frac{x}{a_0}\right), \tag{2.7}$$

$$\frac{p(x,t)}{\rho_0 a_0^2} = f\left(t-\frac{x}{a_0}\right)+f\left(t+\frac{x}{a_0}\right). \tag{2.8}$$

This first-order solution contains the main contribution and is sufficient to describe the flow in the tube for small M.

2.2. *Oscillations near half the fundamental frequency*

The tube considered in §2.1 was driven with a frequency ω close to the fundamental frequency $\pi a_0/L$. In the present section it is driven with $\frac{1}{2}\omega$ and the boundary condition at the piston becomes

$$u(L,t) = u_A \cos\tfrac{1}{2}\omega t. \tag{2.9}$$

In this case the solution given by (1.1) fails, too, as the first overtone, driven by the nonlinear term, becomes resonant. Keller (1975) follows Chester's (1964) theory described in §2.1. In Keller's case a narrow frequency band

$$\tfrac{1}{2}\omega = \frac{\pi a_0}{2L}+\tfrac{1}{2}\Delta\omega, \tag{2.10}$$

with $\Delta\omega/\omega \ll 1$ is considered. The analysis can easily be extended to $\frac{3}{2}\omega$, $\frac{5}{2}\omega$, etc. as long as Mortell & Seymour's (1981) amplitude parameter (proportional to $\omega^2 l L/a_0^2$) remains small. The following splitting that can be made according to Keller (1975) is crucial:

$$f(t) = f_A(t)+f_s(t) \tag{2.11}$$

with

$$\left.\begin{aligned} f_A\left(t-\frac{L_r}{a_0}\right) &= -f_A\left(t+\frac{L_r}{a_0}\right), \\ f_s\left(t-\frac{L_r}{a_0}\right) &= f_s\left(t+\frac{L_r}{a_0}\right), \end{aligned}\right\} \tag{2.12}$$

and with the abbreviations $L_r = \pi a_0/\omega$.

Introducing (2.11) into Chester's (1964) theory leads to the following expression for the non-resonant contribution f_A:

$$u_A \cos\tfrac{1}{2}\omega t = 2a_0 f_A\left(t-\frac{L_r}{a_0}\right)+\tfrac{1}{2}\beta a_0 \int_0^\infty f_A\left(t-\frac{L_r}{a_0}-\xi\right)\xi^{-\frac{1}{2}}\,\mathrm{d}\xi. \tag{2.13}$$

The solution of (2.13), that corresponds to equation (6.9) in Chester's (1964) paper is

$$f_A(t) = -\frac{u_A}{2a_0}\,\frac{\sin\tfrac{1}{2}\omega t+\left(\frac{\pi}{\omega}\right)^{\frac{1}{2}}\frac{\beta}{2\sqrt{2}}\sin\left(\tfrac{1}{2}\omega t+\tfrac{1}{4}\pi\right)}{1+\left(\frac{\pi}{\omega}\right)^{\frac{1}{2}}\tfrac{1}{2}\beta+\frac{\pi}{\omega}\tfrac{1}{8}\beta^2}. \tag{2.14}$$

For vanishing viscosity ($\beta = 0$) this reduces to

$$f_A(t) = -\frac{u_A}{2a_0}\sin\tfrac{1}{2}\omega t. \tag{2.15}$$

The difference between (2.11) and Keller's (1975) equation (8) explains the phase difference of $\frac{1}{2}\pi$ between (2.15) and Keller's result.

The resulting equation for the resonant contribution f_s reads

$$c - f_A^2(t) = -\frac{4r}{\pi}\epsilon^{\frac{1}{2}} f_s(t) + f_s^2(t) - s\left(\frac{\omega\epsilon}{\pi}\right)^{\frac{1}{2}}\int_0^\infty f_s(t-\xi)\,\xi^{-\frac{1}{2}}\,\mathrm{d}\xi, \tag{2.16}$$

which corresponds to Keller's (1975) equation (17). It is very similar to (2.2). The main difference stems from the fact that f in (2.2) is 'driven' by the piston ($\epsilon_c \sin\omega t$) while f_s in (2.16) is 'driven' by the nonlinear effect (f_A^2) of the non-resonant oscillation. Several terms that are negligible for the conditions of the present experiments have been dropped from (2.13) and (2.16). Viscous effects have a very small influence on the non-resonant part f_A for the conditions of the present experiments. Equation (2.15) can therefore be used in (2.16) to determine the second-order quantity f_s. This leads to

$$c + \tfrac{1}{2}\epsilon\cos\omega t = -\frac{4r}{\pi}\epsilon^{\frac{1}{2}} f_s(t) + f_s^2(t) - s\left(\frac{\omega\epsilon}{\pi}\right)^{\frac{1}{2}}\int_0^\infty f_s(t-\xi)\,\xi^{-\frac{1}{2}}\,\mathrm{d}\xi, \tag{2.17}$$

with

$$M = \frac{u_A}{a_0} = \frac{\omega l}{2a_0}, \tag{2.18}$$

$$\epsilon = \tfrac{1}{4}M^2, \tag{2.19}$$

$$r = \frac{\pi\Delta\omega}{(\gamma+1)\,\omega\epsilon^{\frac{1}{2}}}, \tag{2.20}$$

$$s = \frac{2\beta(\pi/\omega\epsilon)^{\frac{1}{2}}}{(\gamma+1)}. \tag{2.21}$$

Equations (2.2) and (2.17) are now identical except for the phase shift in the trigonometric function. Solutions of (2.17) will be compared with experiments in §4.

Here, the inviscid solution ($s = 0$) at resonance ($r = 0$) is given as an illustration. f_A is determined by (2.15), and (2.17) reduces to

$$c + \tfrac{1}{2}\epsilon\cos\omega t = f_s^2. \tag{2.22}$$

The solution that satisfies (2.12), has a vanishing mean value and contains no expansion shocks reads

$$f_s = \pm\tfrac{1}{2}M\cos\tfrac{1}{2}\omega t. \tag{2.23}$$

The change of sign takes place at $\frac{1}{2}\omega t = 0, \pi, 2\pi, \ldots$, with a jump from $-\frac{1}{2}M$ to $+\frac{1}{2}M$. The function $p(0,t) = f_A + f_s$ is similar to figure 4 in Galiev *et al.* (1970).

2.3. *Numerical procedures*

(i) The non-resonant acoustic contributions to $u(x,t)$ and $p(x,t)$ (corresponding to f_A) are of order M, and their calculation deserves therefore the highest possible accuracy.

The solutions given by Iberall (1950) are therefore used, as they contain few assumptions and are not restricted to boundary layers thin compared with the tube radius. With the boundary conditions $u(0,t) = 0$ and $u(L,t) = u_A \cos \omega' t$, and with the abbreviations suggested by Rott (1969), the velocity, averaged over the cross-section, and the pressure disturbance can be written as

$$\frac{u}{u_A} = \frac{\sin(h\omega' x/a_0)}{\sin(h\omega' L/a_0)} \exp(\mathrm{i}\omega' t), \tag{2.24}$$

$$\frac{p}{\rho_0 a_0 u_A} = \frac{\mathrm{i}}{h(1-f_1)} \frac{\cos(h\omega' x/a_0)}{\sin(h\omega' L/a_0)} \exp(\mathrm{i}\omega' t), \tag{2.25}$$

with

$$h = \left(\frac{1+(\gamma-1)f^*}{1-f_1}\right)^{\frac{1}{2}},$$

$$f_1 = \frac{2}{z}\frac{J_1(z)}{J_0(z)}, \quad f^* = f_1(zP\gamma^{\frac{1}{2}}),$$

$$z = \mathrm{i}^{\frac{3}{2}}\left(\frac{\omega' R^2}{\nu_0}\right)^{\frac{1}{2}},$$

$$\mathrm{i} = (-1)^{\frac{1}{2}},$$

$$\omega' = \tfrac{1}{2}\omega,$$

and J_0 and J_1 are the Bessel functions of the first kind. As usual, the real parts are taken as the physical solutions.

(ii) The resonant contribution f_s is of order M. Depending on the value of s different numerical procedures had to be used.

For $0 \leqslant s \leqslant 0.4$, f_s was determined by a modification of (2.17), where the substitutions

$$f_s(t) = \epsilon^{\frac{1}{2}} g(\lambda), \tag{2.26}$$

$$\lambda = \omega t, \tag{2.27}$$

were made. The result is

$$\left\{g(\lambda) - \frac{2r}{\pi}\right\}^2 = c + \tfrac{1}{2}\cos\lambda + \frac{s}{\pi^{\frac{1}{2}}} \int_0^\infty g(\lambda-\sigma)\,\sigma^{-\frac{1}{2}}\,\mathrm{d}\sigma. \tag{2.28}$$

The function $g(\lambda)$ was computed with the following iteration scheme, suggested by Keller (1976*a*):

$$\left\{g_n(\lambda) - \frac{2r}{\pi}\right\}^2 = c_n + \tfrac{1}{2}\cos\lambda + \frac{s}{\pi^{\frac{1}{2}}} \int_0^\infty g_{n-1}(\lambda-\sigma)\,\sigma^{-\frac{1}{2}}\,\mathrm{d}\sigma. \tag{2.29}$$

It is useful to replace the integral with Chester's (1964) equation (6.4),

$$\int_0^\infty g(\lambda-\sigma)\,\sigma^{-\frac{1}{2}}\,\mathrm{d}\sigma = \pi^{-\frac{1}{2}} \int_0^{2\pi} g(\sigma) \sum_{n=1}^{\infty} \frac{\cos(n(\lambda-\sigma) - \frac{1}{4}\pi)}{n^{\frac{1}{2}}}\,\mathrm{d}\sigma. \tag{2.30}$$

The iteration is started with the inviscid solution for g_{n-1}. The constant of integration c_n is determined such that the minimum of the terms on the right-hand side of (2.29) equals zero. At the time of this minimum the solution $g(\lambda)$ is allowed to change from the positive to the negative root of the right-hand side. The position of the shock

(jump from the negative to the positive root) is chosen such that the average of $g(\lambda)$ vanishes. The integration was carried out with 400 points per period.

For $0.4 < s < 1$, slow convergence of the scheme mentioned above was observed. Successive iterations generated shocks located on either side of their final position with a slowly decreasing deviation. The following procedure solved this problem:

$$\left\{g_n(\lambda)-\frac{2r}{\pi}\right\}^2 = c_n+\tfrac{1}{2}\cos\lambda+\frac{s}{\pi^{\frac{1}{2}}}\int_0^\infty \tfrac{1}{2}(g_{n-1}(\lambda-\sigma)+g_{n-2}(\lambda-\sigma))\,\sigma^{-\frac{1}{2}}\,\mathrm{d}\sigma. \quad (2.31)$$

The rest of the procedure was unchanged.

For $s \gg 1$ the nonlinear contribution f_s^2 in (2.17) can be neglected and the arguments leading to (2.14) can also be used here. The result is

$$f_s(t) = -\epsilon^{\frac{1}{2}}\frac{\frac{2r}{\pi}\cos\omega t+\frac{1}{2}s\cos(\omega t+\frac{1}{4}\pi)}{\left(\frac{4r}{\pi}\right)^2+2^{\frac{1}{2}}\frac{4r}{\pi}s+s^2}. \quad (2.32)$$

For the experiments with air, s is as low as 3.8, but (2.32) is still an excellent approximation for the terms with the argument ωt. To show this, (2.32) is inserted into the f_s^2-term in (2.17). An improved f_s is then determined with the remaining linear terms. This solution contains (2.32) and new terms with the argument $2\omega t$. If this procedure is repeated once more, the terms in (2.32) are slightly changed. To show the difference, this improved solution is compared with (2.32) at resonance.

Equation (2.32) predicts a maximum of the $g(\lambda)$ amplitude for

$$\frac{4r}{\pi} = -\frac{s}{\sqrt{2}}, \quad (2.33)$$

and, there, is

$$f_{sr} = \frac{\epsilon^{\frac{1}{2}}}{(\sqrt{2})\,s}\sin\omega t. \quad (2.34)$$

At the resonant frequency, determined by (2.33), the improved solution is

$$f_{sr} = \epsilon^{\frac{1}{2}}\left[\frac{1}{(\sqrt{2})\,s}-\frac{1}{4\sqrt{2}(\sqrt{2}-1)\,s^5}\right]\sin\omega t-\frac{\epsilon^{\frac{1}{2}}}{4(\sqrt{2})\,s^5}\cos\omega t. \quad (2.35)$$

For $s = 3.8$ the differences between the amplitudes and the phases predicted by (2.34) and (2.35) are negligible.

The numerical predictions of this section are compared with the experiments in figures 5–9.

3. Experimental arrangement and test procedure

The experiments were conducted in an aluminium tube with an inner diameter of 20 mm ($R = 10$ mm) and a wall thickness of 2 mm. A pressure transducer was inserted flush into the end plate at $x = 0$. Kistler transducers 7031 and 601 A with eigenfrequencies of 80 and 130 kHz were used for the experiments with heavy gases. Both transducers gave the same results. The pressure signals with air had considerably smaller amplitudes and contained no shocks. A DRUCK PDCR 22 transducer with a lower eigenfrequency of 28 kHz, but with a better resolution, was therefore used in this case. The temperature at $x = 0$, $x = \frac{1}{2}L$ and 96 mm from the piston was measured with thermocouples. The three readings differed at most by 0.4 K, which is in accordance with Merkli & Thomann (1975*b*).

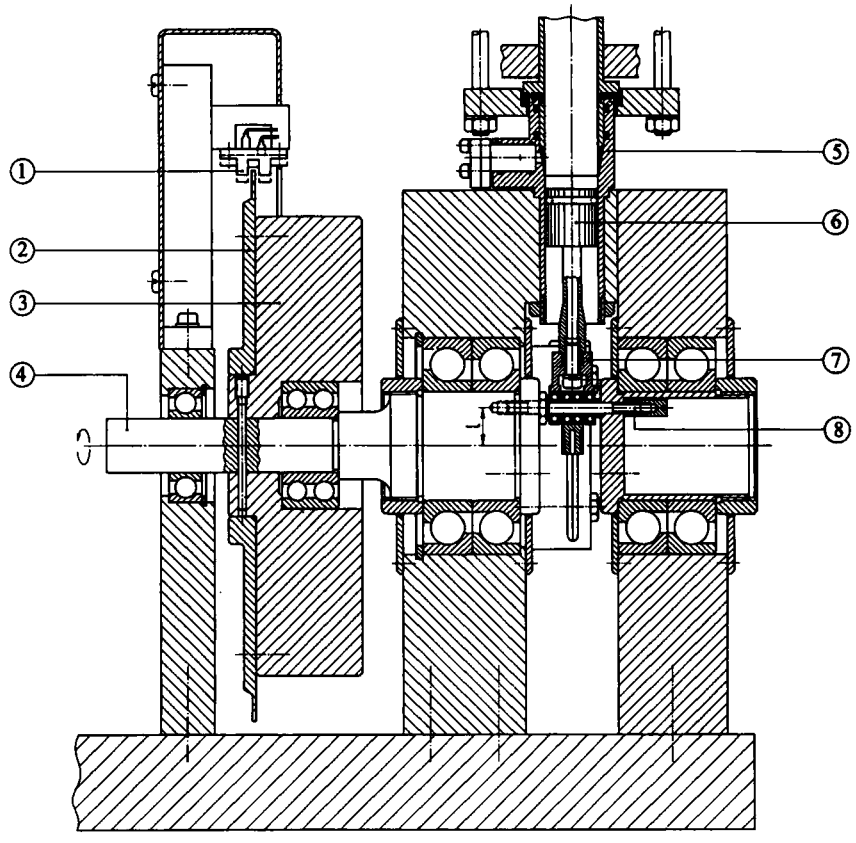

FIGURE 3. Arrangement for the generation of a sinusoidal piston motion.

By far the most crucial part of the present experiment was the arrangement that generated the sinusoidal motion of the piston. It is shown in figures 1 and 3. The rotating part consists of a crankshaft (4) with a crankpin (8) and flywheel (3). A plate (7) with a horizontal slit transferred the rotation into an oscillation of the piston (6). The eccentricity of the crankpin could be changed. It determined the amplitude l of the piston motion. The piston was sealed with an O-Ring and lubricated from below with an oil mist. The position of the piston was determined with a disk (2) with 360 notches and photocells (1). (5) is an elastic connection with the tube. The crankshaft was driven by a d.c. motor with an accurate speed control.

Two effects render the present experiments difficult. First, shocks occur only in a very narrow frequency band with $|r| < 1$. Equation (2.20) leads to $\Delta\omega/\omega = O(l/L)$ for the present subharmonic resonance, while (2.4) predicts a much wider band $\Delta\omega/\omega = O(l/L)^{\frac{1}{2}}$ for the ordinary resonance. Very good speed control is therefore necessary. Relative speed variations observed during one experiment were below 0.2‰. The second and still more critical effect is the second harmonic of the piston motion. It drives the resonant oscillation f_s as the nonlinear, and small, f_A^2 in (2.16) does. If l_2 is the amplitude of the piston motion's second harmonic, and l_{2c} the critical amplitude that has the same effect as f_A^2 has, a comparison of (2.19) with (2.3) leads for $\omega L/a_0 = \pi$ to

$$\frac{l_{2c}}{l} = \tfrac{1}{64}\pi^2(\gamma+1)\frac{l}{L}. \tag{3.1}$$

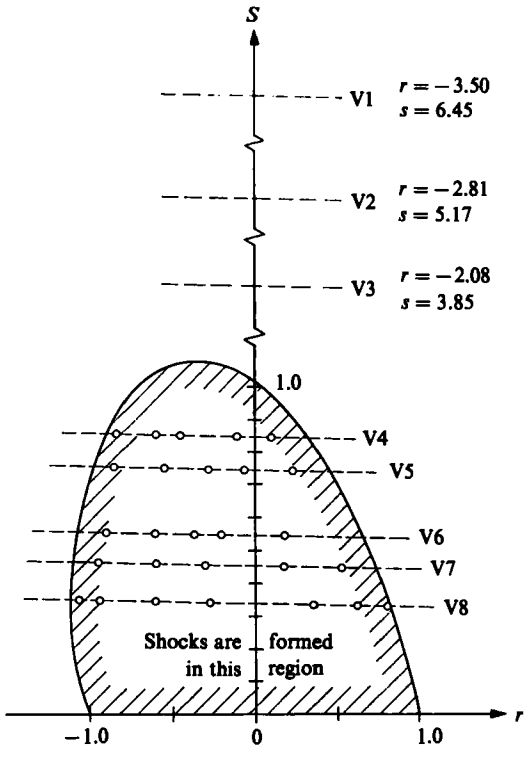

FIGURE 4. Experiments in the (r, s)-plane; r from (2.20) and s from (2.11). Numbers for V1 to V3 are at the resonant frequency.

As $l_2 \ll l_{2c}$ is required, a careful design and test of the piston drive is crucial. The amplitude l_2 was determined with a Kistler 8044 accelerometer attached to the piston. For the smaller piston amplitude ($l = 9.44$ mm) there resulted $l_2 < 0.002$ mm while $l_2 < 0.003$ mm resulted for $l = 12.58$ mm. This leads to upper limits for l_2/l_{2c} and thus for the error of the amplitude of the resonant overtone of 6–8 % for air and of 2–3 % for the other gases. The motion of the closed end of the tube was an order of magnitude smaller than l_2 and can also be neglected.

It can also be shown that the error introduced by neglecting the difference between the real piston velocity $u(x_{\text{piston}}, t)$ and the assumed $u(L, t)$ in (2.9) is negligible for the present conditions, as $\partial u/\partial x(L, t) \approx 0$ for the 'driving' non-resonant acoustic solution.

The tests were conducted in the following way. A fixed frequency close to resonance was chosen and the signal of the pressure transducer was recorded 72 times per period of oscillation during 17 periods, except for xenon where 60 points per period were recorded during 21 periods. The temperature and the frequency were recorded less frequently as their changes during an experiment were negligible. This procedure was repeated for different frequencies.

4. Results

Eight experiments were conducted and their location in the (r, s)-plane is shown in figure 4. Four of them will be presented here; the rest are presented by Althaus (1986). The pertinent parameters for the experiments are given in table 1.

Experiment	V3	V4		V6		V8	
Gas	Air	Xe		SF_6		RC-318	
l (mm)	12.58	12.60		12.58		12.58	
L (m)	1.1556	0.4856		0.4756		0.3956	
p_0 (bar)	0.9521	0.9530		0.9593		0.9426	
T_0 (K)	293.1	292.5		290.9		291.9	
ρ_0 (kg/m^3)	1.127	5.171	(V)	5.867	(D)	8.014	(M)
a_0 (m/s)	343.7	175.3		133.3		111.4	
$\nu_0\,10^{-5}$ m^2/s	1.611	0.4350	(A)	0.2587	(B)	0.1446	(A)
c_p (J/kg.K)	1004.1	160.0	(V)	666.1	(D)	792.7	(M)
Pr	0.7101	0.6380	(A)	0.7494	(B)	0.7510	(A)
γ	1.398	1.667	(B)	1.087	(D)	1.055	(B)
$(a_e-a_0)/a_0$	—	−0.0039		0.0029		−0.0102	
M	0.0171	0.0408		0.0415		0.0500	
A (equation (4.5))	134	359		427		588	

TABLE 1. Numerical data used for the reduction of the experiments, $M = u_A/a_0 = \pi l/2L$ at resonance. The properties of air were calculated with the equations collected by Lommel (1981). [Source of properties: (A), Air Liquide 1976; (B), Braker & Mossman 1976; (D), Döring 1979; (M), Matthias & Löffler 1965; (V), Vargaftik 1975.]

4.1. *Results for air*

In this case the viscosity parameter s at resonance equals 6.45, 5.17 and 3.85 and no shocks are formed. The measured pressure $p(0,t)$ was therefore decomposed into its Fourier components. The piston velocity, the non-resonant first harmonic and the resonant second one are defined by

$$u(L,t) = u_A \cos \tfrac{1}{2}\omega t, \tag{4.1}$$

$$p_1(0,t) = \hat{p}_1 \cos(\tfrac{1}{2}\omega t + \phi_1), \tag{4.2}$$

$$p_2(0,t) = \hat{p}_2 \cos(\omega t + \phi_2), \tag{4.3}$$

with $u_A = \frac{1}{2}\omega l$.

The results for the first harmonic are shown in figure 5. The difference between the experiment and the linear theory (equation (2.25)) is less than 0.4 %, which is within the experimental accuracy.

The resonant second harmonic is driven by nonlinear effects, and it would vanish if they did not exist. The good agreement between the experiment and the theory shown in figure 6 is therefore a good confirmation of Keller's (1975) theory. The difference between the experimental and the theoretical maximum of the amplitude is 2 % and supports the accuracy of the piston motion indicated in §3. For experiment V3 the amplitudes $\hat{p}/\rho_0 a_0 u_A$ were, for the first to the sixth harmonic respectively, 1.004/0.187/0.0036/0.0137/0.00067 and 0.00141. The discrepancy in the phase ϕ_2 cannot be explained with experimental errors, as ϕ_1 in figure 5 is correct.

4.2. *Results for the heavy gases*

Shock waves formed in this case in a very narrow frequency band. The position of the shock on the first harmonic (figures 7–9) allows a very accurate determination of an experimental resonant frequency

$$\omega_e = \frac{\pi a_e}{L}, \tag{4.4}$$

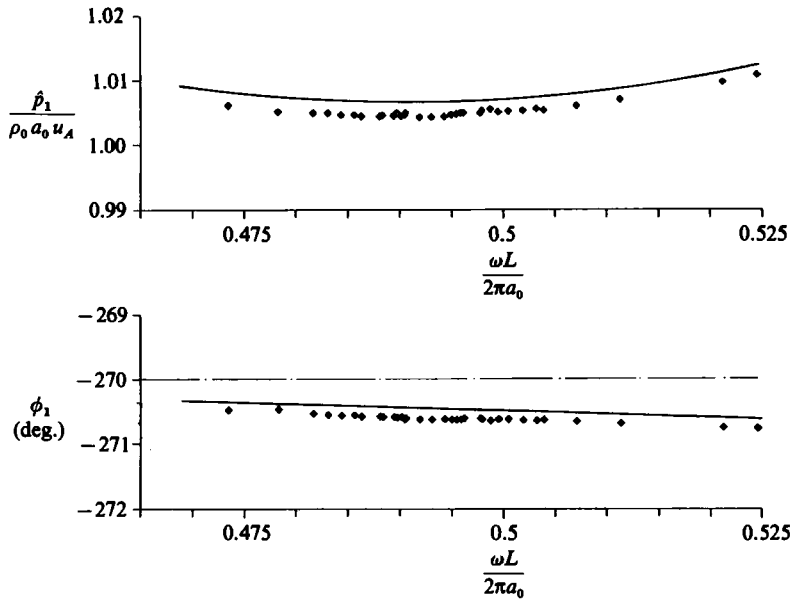

FIGURE 5. Amplitude and phase of first harmonic, experiment V3, parameters in table 1, ——, equation (2.25).

close to $\pi a_0/L$, where a_e is a fictitious speed of sound near $a_0 = (\gamma p_0/\rho_0)^{\frac{1}{2}}$. For the comparison with theory, a_e was used to determine $\Delta\omega$ in (2.10) and (2.20). The small differences $(a_e - a_0)/a_0$ are given in table 1 for the different experiments. As they are fairly constant for a given gas and of different signs for different gases, it is likely that the corrections are mainly due to small errors in the speed of sound calculated from γ, p_0 and ρ_0 predicted by the literature, and to higher-order non-linear effects not taken into account in Keller's (1975) theory.

The experiments are compared with theoretical predictions in figures 7–9. Five different frequencies are shown, with number 3 closest to resonance. Excellent agreement is again observed. The first harmonic of the signals was compared with (2.25). For Xe and SF_6 the deviation was 0.3 %, while for Freon it was 1.4 %.

The need for higher-order corrections of the theory, as considered by Keller (1976*b*), are indicated by the small asymmetry of the pressure signals. The experiments are above the theoretical curve both at the pressure maximum and at the minimum, and the deviation increases with decreasing viscosity parameter.

Experiments by Merkli & Thomann (1975*a*) and Stuhlträger & Thomann (1986) with the same equipment showed that the boundary layer on the tube wall becomes turbulent if

$$A = \frac{2\hat{u}}{(\omega' \nu_0)^{\frac{1}{2}}} \geqslant 350 \text{ to } 750 \tag{4.5}$$

where $\hat{u}$ is the local velocity amplitude and $\omega' = \frac{1}{2}\omega$ is the frequency of the piston motion.

Numbers for the present experiments are given in table 1. Some turbulence might have been present for V8, but a comparison of the signals in figure 9 with the other results shows that the influence of turbulence is negligible.

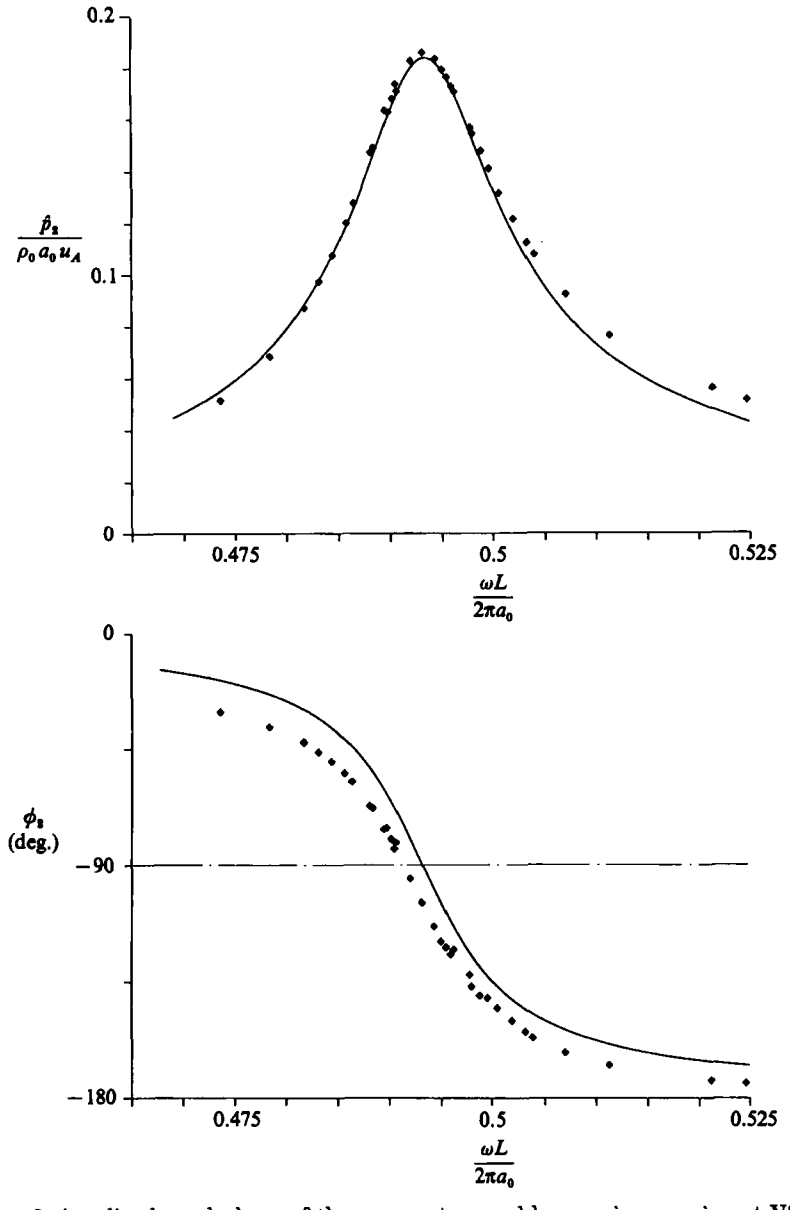

FIGURE 6. Amplitude and phase of the resonant second harmonic, experiment V3, parameters in table 1, ——, equation (2.32).

5. Conclusions

The first overtone, driven by nonlinear effects, becomes resonant near half the fundamental frequency. The amplitude of this resonant contribution is comparable to the non-resonant linear solution as shown in figure 2. This resonant peak is very narrow and more strongly damped by viscous effects. The present experiments show that Keller's (1975) theory predicts these effects very well. Unexplained is the discrepancy in the phase in figure 6.

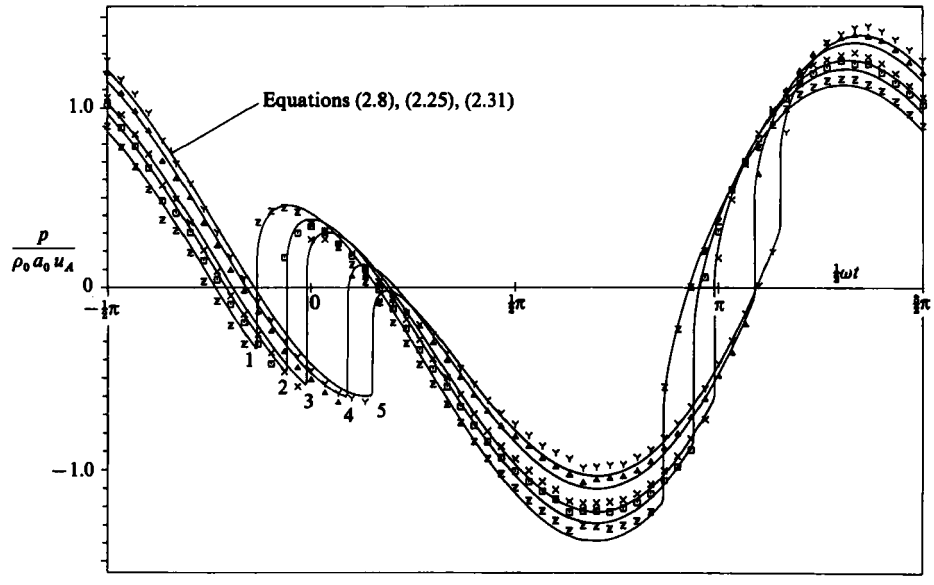

FIGURE 7. Pressure at the closed end for xenon, experiment V4, parameters in table 1. 1: $r = -0.840$, $s = 0.856$; 2: $r = -0.601$, $s = 0.853$; 3: $r = -0.450$, $s = 0.851$; 4: $r = -0.116$, $s = 0.840$; 5: $r = 0.101$, $s = 0.836$.

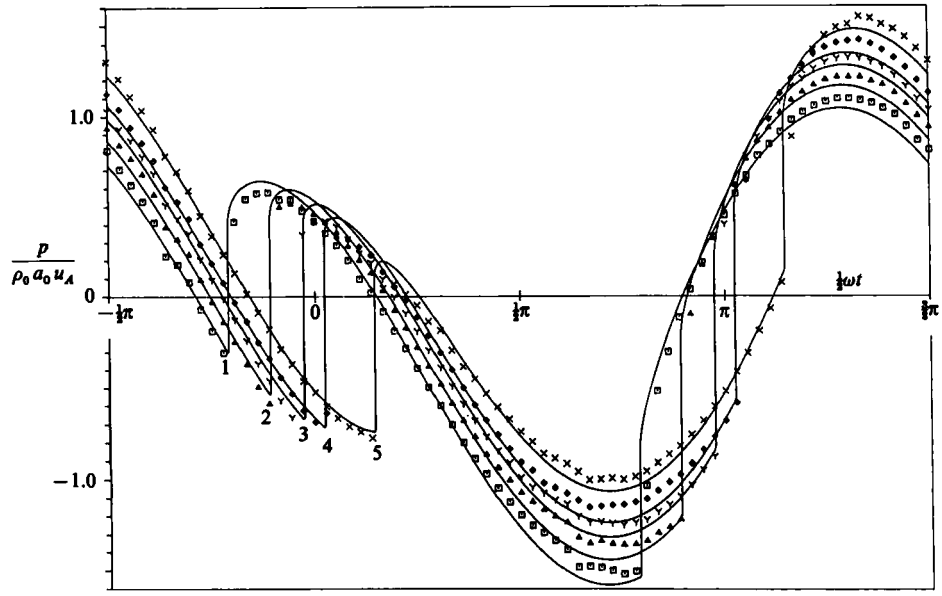

FIGURE 8. Pressure at the closed end for SF_6, experiment V6. 1: $r = -0.904$, $s = 0.558$; 2: $r = -0.626$, $s = 0.554$; 3: $r = -0.368$, $s = 0.552$; 4: $r = -0.198$, $s = 0.549$; 5: $r = 0.182$, $s = 0.544$.

Similar effects are predicted by Keller (1976*b*) for multiples $\frac{1}{3}$, $\frac{2}{3}$ etc. of the fundamental frequency. In this case, however, they remain well below the non-resonant signal and are difficult to detect. Figure 10 shows the results of an experiment with Freon R 114 ($l = 12.58$ mm, $L = 0.407$ m, $3\omega L/\pi a_0 \approx 0.995$). An indication of three shocks is clearly visible. No reduction of the data was made, as

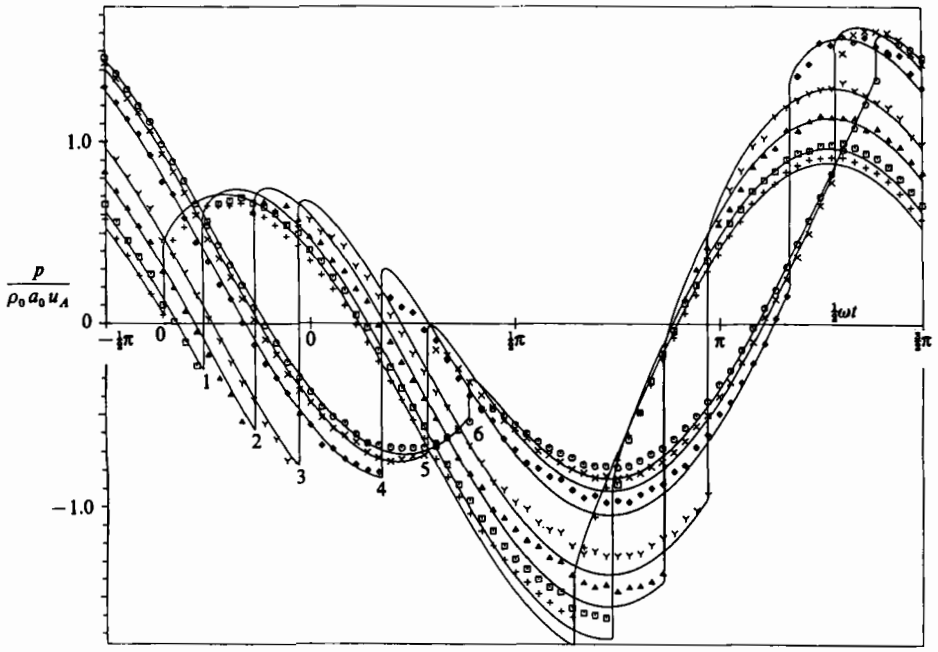

FIGURE 9. Pressure at the closed end for Freon RC-318, experiment V8. 0: $r = -1.076$, $s = 0.348$; 1: $r = -0.940$, $s = 0.347$; 2: $r = -0.596$, $s = 0.344$; 3: $r = -0.271$, $s = 0.342$; 4: $r = 0.360$, $s = 0.335$; 5: $r = 0.636$, $s = 0.334$; 6: $r = 0.810$, $s = 0.332$.

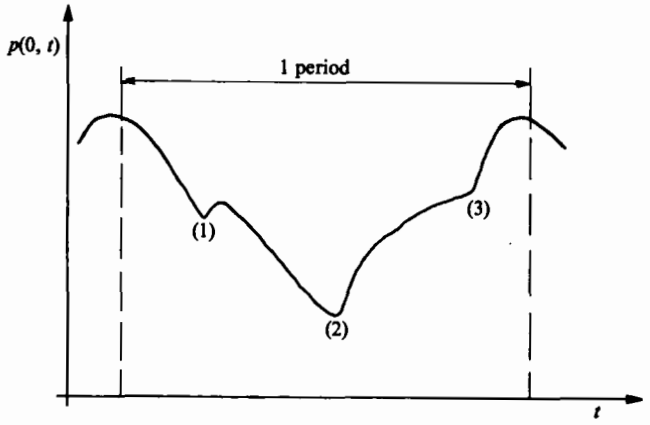

FIGURE 10. Pressure signal near $\frac{1}{3}$ of the fundamental frequency. Shocks at (1), (2) and (3).

the frequency band is still more narrow and the requirements on the precision of piston drive are more severe.

It was pointed out by Rott (1980) that similar effects can be expected at any rational fraction of the fundamental frequency. As these higher-order effects are more strongly damped by viscosity, they will not show up unless the kinematic viscosity is extremely small, which is the case at high pressures.

REFERENCES

AIR LIQUIDE 1976 *Gas Encyclopedia*. Elsevier.

ALTHAUS, R. 1986 Experimentelle Untersuchung resonanter subharmonischer Schwingungen einer Gassäule in einem geschlossenen Rohr. Diss. *ETH Zürich* no. 8098.

BRAKER, W. & MOSSMAN, A. L. 1976 *The Matheson Unabridged Gas Data Book*. Matheson.

CHESTER, W. 1964 Resonant oscillations in closed tubes. *J. Fluid Mech.* **18**, 44.

DÖRING, R. 1979 *Schwefelhexafluorid (SF_6) Dampftafel im internationalen Einheitssystem*. Hannover: Kali-Chemie.

GALIEV, S. U., ILHAMOV, M. A. & SADYKOV, A. V. 1970 Periodic shock waves in a gas. *Isv. Akad. Nauk SSSR. Mech. Zhid. i Gaza* **5**, 57–66.

GALIULLIN, R. G. & KHALIMOV, G. G. 1979 Investigation of nonlinear oscillations of a gas in open pipes. *J. Engng Phys.* (*USSR*) **37**, 1439.

IBERALL, A. S. 1950 Attenuation of oscillatory pressures in instrumental lines. *J. Res. Natl Bur. Stand.* **45**, 85.

KELLER J. J. 1975 Subharmonic non-linear acoustic resonances in closed tubes. *Z. angew. Math. Phys.* **26**, 395.

KELLER, J. J. 1976*a* Resonant oscillations in closed tubes. *J. Fluid Mech.* **77**, 279.

KELLER, J. J. 1976*b* Third order resonances in closed tubes. *Z. angew. Math. Phys.* **27**, 303.

KELLER, J. J. 1977 Subharmonic non-linear acoustic resonances in open tubes. Part 1: Theory. *Z. angew. Math. Phys.* **28**, 419.

LOMMEL, A. 1981 Ausbreitung schwacher Expansionswellen in einem engen langen Rohr. Diss. *ETH Zürich* no. 6898.

MATTHIAS, H. & LÖFFLER, H. J. 1965 Thermodynamische Eigenschaften von Octafluorcyclobutan C_4F_8 (RC-318).

MERKLI, P. & THOMANN, H. 1975*a* Transition to turbulence in oscillating pipe flow. *J. Fluid Mech.* **68**, 567.

MERKLI, P. & THOMANN, H. 1975*b* Thermoacoustic effects in a resonance tube. *J. Fluid Mech.* **70**, 161.

MORTELL, M. P. & SEYMOUR, B. R. 1981 A finite-rate theory of quadratic resonance in a closed tube. *J. Fluid Mech.* **112**, 411.

ROTT, N. 1969 Damped and thermally driven acoustic oscillations in wide and narrow tubes. *Z. angew. Math. Phys.* **20**, 230.

ROTT, N. 1980 Nichtlineare Akustik – Rückblick und Ausblick. *Z. Flugwiss. Weltraumforschung* **4**, 185.

ROTT, N. 1980 Non-linear acoustics. *Proc. Intl Congr. of Theoret. Appl. Mech. Toronto.*

STUHLTRÄGER, E. & THOMANN, H. 1986 Oscillations of a gas in an open-ended tube near resonance. *Z. angew. Math. Phys.* **37**, 155.

STURTEVANT, B. & KELLER, J. J. 1978 Subharmonic nonlinear acoustic resonances in open tubes, Part II: Experimental investigation of the open-end boundary condition. *Z. angew. Math. Phys.* **29**, 473.

VARGAFTIK, N. B. 1975 *Tables on the Thermophysical Properties of Liquids and Gases*. Hemisphere.

ZARIPOV, R. G. & ILHAMOV, M. A. 1976 Nonlinear gas oscillations in a pipe. *J. Sound Vib.* **46**, 245.